Title

Loss of Cellulose synthase-like F6 function affects mixed-linkage glucan deposition, cell wall mechanical properties, and defense responses in vegetative tissues of rice.

Journal

Plant physiology, 159(1)

ISSN

1532-2548

Authors

Vega-Sánchez, Miguel E
Verhertbruggen, Yves
Christensen, Ulla
et al.

Publication Date

2012-05-02

Peer reviewed

Loss of *Cellulose Synthase-Like F6* Function Affects Mixed-Linkage Glucan Deposition, Cell Wall Mechanical Properties, and Defense Responses in Vegetative Tissues of Rice[1][C][W][OA]

Miguel E. Vega-Sánchez, Yves Verhertbruggen, Ulla Christensen, Xuewei Chen[2], Vaishali Sharma, Patanjali Varanasi, Stephen A. Jobling, Mark Talbot, Rosemary G. White, Michael Joo, Seema Singh, Manfred Auer, Henrik V. Scheller, and Pamela C. Ronald*

Joint BioEnergy Institute, Emeryville, California 94608 (M.E.V.-S., Y.V., U.C., X.C., V.S., P.V., M.J., S.S., M.A., H.V.S., P.C.R.); Divisions of Physical Biosciences (Y.V., U.C., V.S., H.V.S., P.C.R.) and Life Sciences (M.J., M.A.), Lawrence Berkeley National Laboratory, Berkeley, California 94720; Commonwealth Scientific and Industrial Research Organization Food Futures Flagship (S.A.J., M.T., R.G.W.) and Commonwealth Scientific and Industrial Research Organization Plant Industry (S.A.J.), Black Mountain Laboratories, Black Mountain, Australian Capital Territory 2601, Australia; Department of Plant Pathology (M.E.V.-S., X.C., P.C.R.) and The Genome Center (P.C.R.), University of California, Davis, California 95616; Biomass Science and Conversion Technologies Department, Sandia National Laboratories, Livermore, California 94551 (P.V., S.S.); and Department of Plant Molecular System Biotechnology and Crop Biotech Institute, Kyung Hee University, Yongin 446–701, Korea (P.C.R.)

Mixed-linkage glucan (MLG) is a cell wall polysaccharide containing a backbone of unbranched (1,3)- and (1,4)-linked β-glucosyl residues. Based on its occurrence in plants and chemical characteristics, MLG has primarily been associated with the regulation of cell wall expansion due to its high and transient accumulation in young, expanding tissues. The *Cellulose synthase-like F* (*CslF*) subfamily of glycosyltransferases has previously been implicated in mediating the biosynthesis of this polymer. We confirmed that the rice (*Oryza sativa*) *CslF6* gene mediates the biosynthesis of MLG by overexpressing it in *Nicotiana benthamiana*. Rice *cslf6* knockout mutants show a slight decrease in height and stem diameter but otherwise grew normally during vegetative development. However, *cslf6* mutants display a drastic decrease in MLG content (97% reduction in coleoptiles and virtually undetectable in other tissues). Immunodetection with an anti-MLG monoclonal antibody revealed that the coleoptiles and leaves retain trace amounts of MLG only in specific cell types such as sclerenchyma fibers. These results correlate with the absence of endogenous MLG synthase activity in mutant seedlings and 4-week-old sheaths. Mutant cell walls are weaker in mature stems but not seedlings, and more brittle in both stems and seedlings, compared to wild type. Mutants also display lesion mimic phenotypes in leaves, which correlates with enhanced defense-related gene expression and enhanced disease resistance. Taken together, our results underline a weaker role of MLG in cell expansion than previously thought, and highlight a structural role for MLG in nonexpanding, mature stem tissues in rice.

[1] This work was supported by the Office of Science, Office of Biological and Environmental Research, of the U.S. Department of Energy (contract no. DE–AC02–05CH11231) and by the Commonwealth Scientific and Industrial Research Organization Food Futures Flagship.

[2] Present address: Rice Institute, Sichuan Agricultural University at Chengdu, 211 Huimin Road, Liucheng, Wenjiang, Chengdu, Sichuan, 611130, China.

* Corresponding author; e-mail pcronald@ucdavis.edu.

The author responsible for distribution of materials integral to the findings presented in this article in accordance with the policy described in the Instructions for Authors (www.plantphysiol.org) is: Pamela C. Ronald (pcronald@ucdavis.edu).

[C] Some figures in this article are displayed in color online but in black and white in the print edition.

[W] The online version of this article contains Web-only data.

[OA] Open Access articles can be viewed online without a subscription.

www.plantphysiol.org/cgi/doi/10.1104/pp.112.195495

Plant primary cell walls are typically composed of cellulose, matrix polysaccharides, and proteins. Among vascular plants, grasses, such as rice (*Oryza sativa*), have unique primary cell walls with a low content of xyloglucan and pectins, and high levels of feruloylated arabinoxylans and (1,3; 1,4)-β-D-glucan (Carpita, 1996; Smith and Harris, 1999; Vogel, 2008), also known as mixed-linkage glucan (MLG). MLG is a polysaccharide containing a backbone of unbranched (1,3)- and (1,4)-linked β-glucosyl residues. In flowering plants, MLG is only found in cell walls of the taxonomic order Poales, which consists of 16 families including the Poaceae (Smith and Harris, 1999; Trethewey et al., 2005). MLG is also found in a few ascomycete fungi (Honegger and Haisch, 2001; Pettolino et al., 2009) and in some species of bryophytes, pteridophytes, and green algae (Popper and Fry, 2003; Fry et al., 2008; Sørensen et al., 2008). The

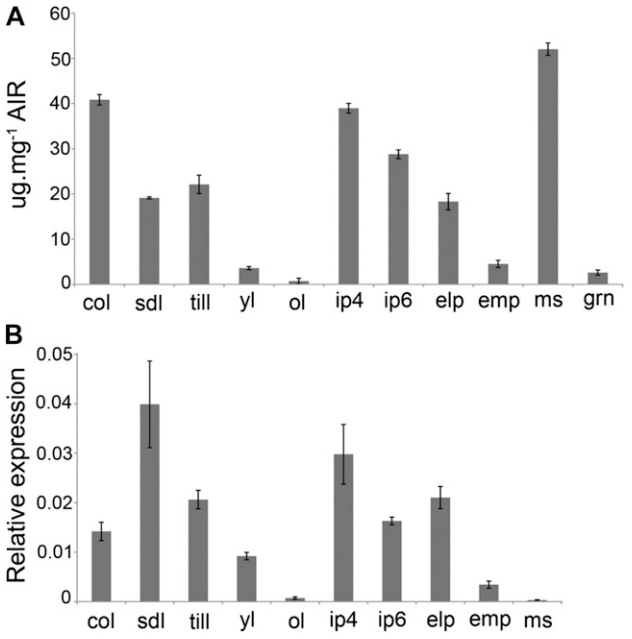

Figure 1. MLG content and *CslF6* expression in rice. A, MLG accumulation throughout development and in different tissues of rice cultivar Nipponbare. B, Quantitative reverse transcription-PCR showing *CslF6* expression in rice tissues throughout development. col, Coleoptile (3-d-old); sdl, seedling (7-d-old); till, tiller (30-d-old); yl, young leaf (30-d-old); ol, old leaf (30-d-old); ip4, immature panicle (4 cm); ip6, immature panicle (6 cm); elp, elongated panicle (11 cm); emp, emerging panicle; ms, mature stem (80-d-old); grn, mature seed (grain).

rare occurrence of MLG among angiosperms and a few divergent species suggests that its adoption evolved independently in all these lineages (Burton and Fincher, 2009; Fincher, 2009a).

MLG has primarily been implicated in the regulation of cell wall expansion due to its high and transient accumulation in young, expanding tissues in the coleoptile and seedling (Carpita et al., 2001; Gibeaut et al., 2005; Christensen et al., 2010). However, MLG also accumulates in cells that are not typically associated with growing tissues such as fibers and xylem vessels in the leaf (Trethewey and Harris, 2002; Doblin et al., 2009), which contain thick, lignified, secondary cell walls that provide structural and mechanical support. Another important role of MLG is as a storage compound particularly in barley (*Hordeum vulgare*), oats (*Avena sativa*), and *Brachypodium distachyon* grains where levels can represent as much as 70% to 80% of the endosperm cell wall (Fincher, 2009b; Guillon et al., 2011). In contrast to other cereals, rice does not accumulate significant amounts of MLG in the grain (Shibuya et al., 1985; Demirbas, 2005).

Two grass-specific subfamilies in the *Cellulose synthase-like* (*Csl*) superfamily of glycosyltransferases have recently been shown to mediate the biosynthesis of MLG: *CslF* and *CslH* (Burton et al., 2006; Doblin et al., 2009). These studies demonstrated the involvement of these gene families in MLG biosynthesis by overexpressing the rice *CslF2* and *CslF4* (Burton et al., 2006) and the barley *CslH1* genes (Doblin et al., 2009) in Arabidopsis (*Arabidopsis thaliana*), a host that does not normally accumulate MLG. These results were later confirmed in grasses by expressing several *CslF* genes under the control of constitutive and endosperm-specific promoters in barley (Burton et al., 2011). In rice, *CslF* and *CslH* are represented as small gene families with eight and three members, respectively (Hazen et al., 2002). Whether the biosynthesis of MLG requires one or more of these proteins acting alone or

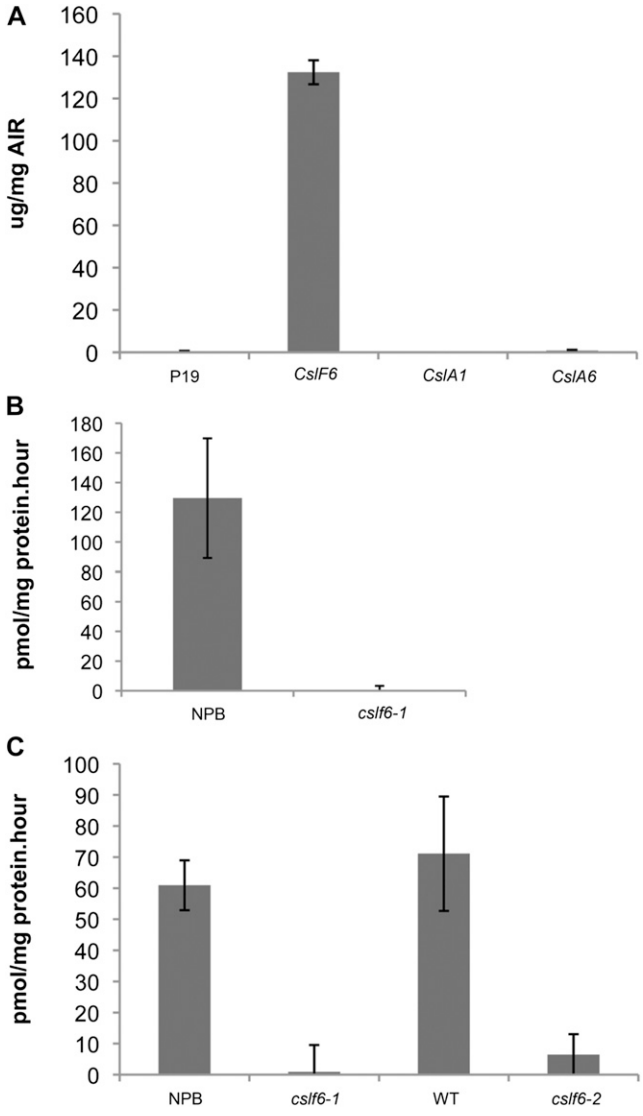

Figure 2. *CslF6* mediates biosynthesis of MLG. A, Accumulation of MLG in *N. benthamiana* leaves following agroinfiltation of constructs overexpressing *CslF6*. p19 (viral silencing suppressor), *CslA1*, and *CslA6* are negative controls. B and C, Endogenous MLG synthase activity assay using purified microsomal fractions from 7-d-old rice seedlings and 4-week-old sheaths, respectively, from wild-type and *cslf6* mutants. NPB, Nipponbare (wild type); WT, segregant of *cslf6-2* without the insertion; $n = 3$ biological replicates; error bars: SEM.

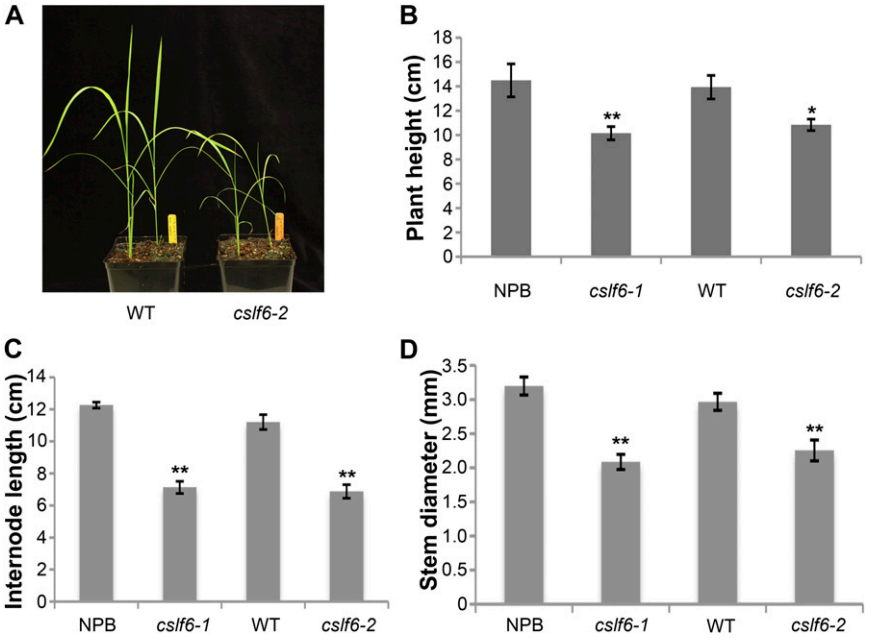

Figure 3. *cslf6* mutant anatomical phenotypes. A, Three-week-old plants. B, Height of 3-week-old plants. $n = 10$; error bars: SEM. C, Second internode length of mature plants after flowering. $n = 8$, error bars: SEM. D, Stem diameter of mature plants after flowering. $n = 8$; error bars: SEM; WT, Segregating sibling of *cslf6-2* without the insertion. Asterisks indicate statistically significant differences at $P < 0.05$ (*) and $P < 0.01$ (**) using Student's *t* test. [See online article for color version of this figure.]

as part of catalytic complexes still needs to be determined. Nevertheless, recent evidence from barley suggests that distinct *CslF* members might mediate the biosynthesis of MLG with different physicochemical properties that may affect the polysaccharide's solubility (Burton et al., 2011).

Despite recent progress in the identification of the genes responsible for MLG biosynthesis in grasses, a detailed understanding of the role of this polysaccharide in any species is still lacking due to the scarcity of characterized mutants. Down-regulation of the *CslF6* gene by RNAi in wheat (*Triticum aestivum*) grain resulted in decreased MLG levels in the endosperm, but has been reported as an industrial application to modulate MLG levels in the grain (Nemeth et al., 2010). Mutations resulting in the absence of MLG accumulation have recently been mapped to the *CslF6* locus in barley (Taketa et al., 2011). However, the characterization of the phenotype was limited to the endosperm and a few tissues in the seedling, and did not discuss or provide evidence for the implications of the absence of MLG in maintaining cell wall integrity (Tonooka et al., 2009; Taketa et al., 2011). Here, we present a detailed analysis of the effects of loss-of-function mutations in the *CslF6* gene in rice vegetative tissues. We show that *CslF6* is required for MLG accumulation in nonlignified, primary cell walls of rice, and necessary and sufficient for MLG deposition in lignified cells of mature stems but not coleoptiles, developing, or expanded leaves. Mutant plants showed a slight growth defect but otherwise grew normally during vegetative development. We also show that mutations in *CslF6* affect the mechanical properties of the cell wall in seedlings and stems, and cause up-regulation of defenses and enhanced resistance to a bacterial pathogen. Taken together, our results provide unequivocal evidence for the predominant role of *CslF6* in MLG biosynthesis in rice and support a cell wall model in which MLG acts as a gel matrix component rather than a cross-linking polysaccharide.

RESULTS

Rice Accumulates MLG throughout Development

There are very few reports on the content of MLG in most rice tissues (Shibuya et al., 1985; Chen et al., 1999;

Table I. *Average cell and inner vascular bundle dimensions in rice stems*[a] and coleoptiles

$n = 400$ and 866 cells for *cslf6* and NPB coleoptiles, respectively; $n = 20$ (vascular bundles), $n = 120$ cells for parenchyma and sclerenchyma. NPB, Nipponbare wild type. Asterisks (**) indicate statistically significant at $P < 0.001$ (Student's *t* test).

Sample	NPB[b]	*cslf6-1*[b]
	μm	
Coleoptile longitudinal sections		
Cell length	39 ± 17.0	29 ± 8.0**
Mature stem cross sections		
Vascular bundle tangential diameter	143.2 ± 17.1	145 ± 17.3
Vascular bundle radial diameter	104.8 ± 11.6	88.3 ± 6.1
Subepidermal sclerenchyma cells	5.6 ± 1.6	4.3 ± 1.7**
Parenchyma cells (first layer)	15.6 ± 14.1	14.9 ± 7.9
Parenchyma cells (excluding first layer)	37.4 ± 13.3	29.0 ± 12.2**

[a]See Figure 5K. [b]Measurement in micrometers ± SD.

Table II. *Oligosaccharide composition from MLG hydrolyzed by lichenase and extracted from different tissues as determined by HPAEC*

Relative amount calculated by adding total tri- and tetrasaccharide amounts. ND, Not detected; NPB, Nipponbare wild type; WT, wild-type segregant without the insertion.

Sample	G4G3G	G4G4G3G	Relative Amount
	μg/mg of AIR		*%*
Coleoptile			
NPB	44.0 ± 0.4	26.0 ± 0.1	100
cslf6-1	1.5 ± 0.1	0.7 ± 0.1	3
cslf6-2	1.5 ± 0.1	0.7 ± 0.02	3
Seedling			
NPB	51.6 ± 0.3	32.5 ± 0.1	100
cslf6-1	Trace	Trace	Trace
WT	60.9 ± 0.1	36.8 ± 0.1	100
cslf6-2	Trace	Trace	Trace
Immature panicle			
NPB	35.1 ± 0.1	24.0 ± 0.1	100
cslf6-1	Trace	Trace	Trace
WT	20.8 ± 1.6	12.0 ± 1.0	100
cslf6-2	Trace	Trace	Trace
Mature stem			
NPB	63.7 ± 3.8	35.2 ± 0.1	100
cslf6-1	Trace	Trace	Trace
WT	59.0 ± 0.6	35.0 ± 1.0	100
cslf6-2	Trace	ND	Trace

Demirbas, 2005; Kimpara et al., 2008). The levels of MLG in crude cell wall preparations (alcohol insoluble residue [AIR]) of different tissues throughout rice development were determined using a commercial assay specific for MLG. As shown in Figure 1A, MLG accumulates in young and mature organs, mostly in younger, rapidly expanding organs such as the coleoptile, seedlings, and immature panicle, which is in agreement with previous reports in maize (*Zea mays*) and barley (Carpita et al., 2001; Gibeaut et al., 2005). Interestingly, the highest MLG content was observed in mature stems after flowering, a tissue containing nonexpanding cells with lignified, secondary cell walls. As opposed to many other grasses, we confirmed that rice does not accumulate significant amounts of MLG in grains (Fig. 1A).

CslF6 Is Predominantly Expressed in Young, Expanding Tissues

A previous gene expression profiling analysis done on 33 rice tissue samples and two rice cultivars revealed that among the *CslF* subfamily, *CslF6* was the most widely and highly expressed family member (Wang et al., 2010). We confirmed these results by extending this analysis using databases of publicly available rice gene expression data that include microarray experiments encompassing 38 rice cultivars and over 1,100 hybridizations (rice oligo array database: http://www.ricearray.org/index.shtml) and the rice MPSS (for Massively Parallel Signature Sequencing) database http://mpss.udel.edu/#rice; Supplemental Fig. S1). A gene expression analysis done in the same tissues used for MLG accumulation above revealed that, although *CslF6* expression did not completely correlate with MLG levels throughout development, it was most highly expressed in young vegetative and reproductive tissues (Fig. 1B).

CSLF6 Mediates the Biosynthesis of MLG

To demonstrate that the rice *CslF6* gene can mediate the biosynthesis of MLG in planta, we transiently overexpressed *CslF6* in leaves of *Nicotiana benthamiana*, a host that does not accumulate MLG. Leaves expressing *CslF6* accumulated remarkably high levels of MLG (about 13% [w/w] of the cell wall preparations), indicating that this gene encodes an MLG synthase (Fig. 2A).

Identification of *cslf6* Knockout Mutants

We had previously identified *CslF6* (MSU ID LOC_Os08g06380; RAP ID Os08g0160500) as a highly expressed, grass-diverged glycosyltransferase using a phylogenomic approach (Cao et al., 2008). The *CslF6* open reading frame is 3.9 kb, encoding for a protein of 952 amino acid residues with nine predicted transmembrane domains and central core catalytic domain typical of members of the CESA (for Cellulose Synthase) superfamily (Supplemental Fig. S2B). Through searches on the Rice Functional Genomic Express database (http://signal.salk.edu/cgi-bin/RiceGE), we identified two independent transposon insertion lines within the *CslF6* genomic sequence: one located in the first intron (TT76-19-6-1: *cslf6-1*) and the other on the last exon (TT76-27-6-17: *cslf6-2*; Supplemental Fig. S2A). Reverse transcription-PCR analysis indicated that *cslf6-1* and *cslf6-2* are knockout lines since no

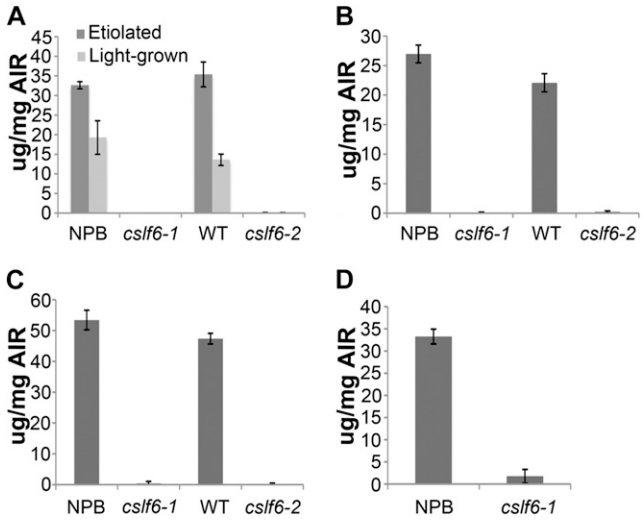

Figure 4. MLG accumulation in *cslf6* mutant. MLG content in 7-d seedlings (A), immature panicles (B), mature stems after flowering (C), and coleoptiles (D). NPB, Nipponbare (wild type); WT, segregant of *cslf6-2* without the insertion.

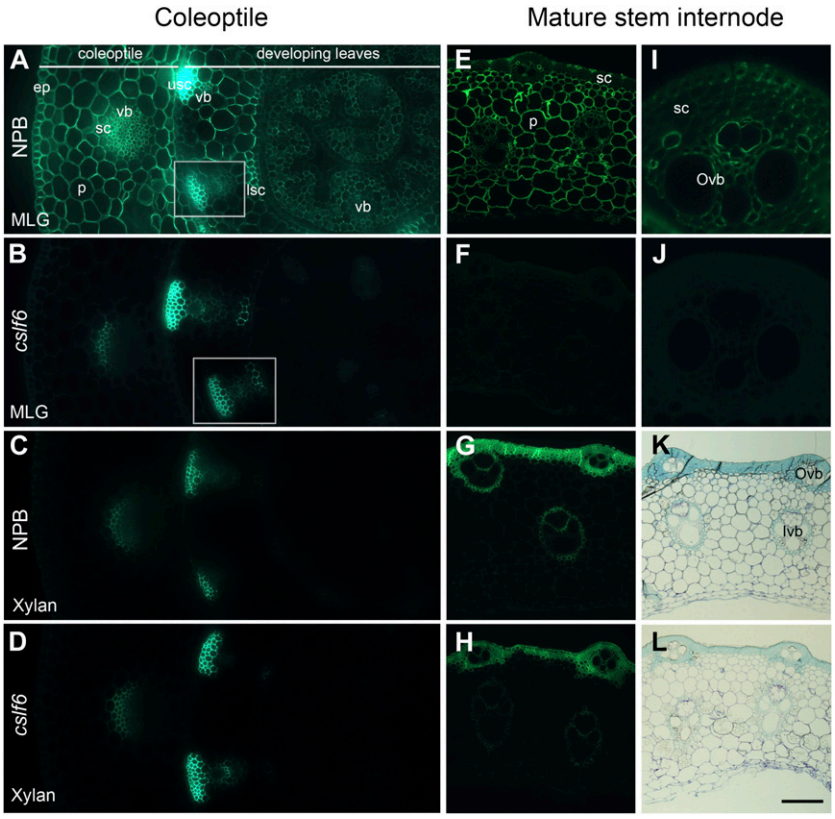

Figure 5. Immunolabeling and staining of coleoptile and stem sections. Wild type (A) and *cslf6* (B) coleoptile sections labeled with anti-MLG monoclonal antibody. Inset: Low exposure micrograph of vascular bundles is shown for clear depiction of cell types in the bundles. Wild-type (C) and *cslf6* (D) coleoptile sections labeled with LM10 xylan antibody. Wild-type (E) and *cslf6* (F) stem internode sections labeled with anti-MLG antibody. Wild-type (G) and *cslf6* (H) stem sections labeled with LM10 antibody. Close-up of wild type (I) and *cslf6* (J) stem sections of the sclerenchyma labeled with anti-MLG antibody. Toluidine blue staining of wild-type (K) and *cslf6* mutant (L) stems showing the presence of secondary cell wall thickenings (light blue). ep, Epidermis; p, parenchyma; sc, sclerenchyma; vb, vascular bundle; usc, upper sclerenchyma; lsc, lower sclerenchyma; ivb, inner vascular bundle; ovb, outer vascular bundle. Scale bar: A to D, 50 μm; E to H, 70 μm; I and J, 15 μm; K and L, 65 μm.

CslF6 transcript could be detected in plants homozygous for the insertions (Supplemental Fig. S2, C and D).

Morphological Phenotypes of *cslf6* Mutants

Homozygous insertion lines for *cslf6-1* and *cslf6-2* were selected and grown under controlled conditions in growth chambers. The *cslf6* mutants did not show any gross morphological phenotypes throughout development. Upon closer inspection, however, we observed that *cslf6* plants are moderately reduced in stature compared to wild-type plants 3 weeks after germination (33% decrease in height; Fig. 3, A and B). The decrease in height correlated with a similar percentage of reduction in cell elongation of 3-d-old coleoptiles: Elongated cells in longitudinal sections from *cslf6-1* coleoptiles were significantly shorter compared to wild type (Table I). At maturity, this growth phenotype was manifested by significantly shorter stem internodes and reduced stem internode diameter, compared to controls (Fig. 3, C and D). The thinner stems in the mutant were primarily due to a reduction in the cross-sectional diameter of sclerenchyma fibers and parenchyma cells compared to wild type (Table I). In contrast, we did not observe changes in diameter or morphology of outer and inner vascular bundles (Table I). Although both *cslf6* mutants showed seemingly normal inflorescence development, anthesis was compromised that resulted in more than 50% reduced seed set (Supplemental Fig. S3A). A closer analysis revealed that although spikelet size was normal (Supplemental Fig. S3B), *cslf6* mutants had deformed anthers and filaments (Supplemental Fig. S3C), suggesting that the poor seed set in the mutant was due to partial male sterility.

With the Exception of Coleoptiles and Leaves, MLG Content and Synthase Activity Are Undetectable in *cslf6* Mutants

To assess whether mutations in *CslF6* had any effect on MLG accumulation, we measured the polysaccharide content in cell wall samples from wild type and mutants. High-performance anion-exchange chromatography (HPAEC) analysis of oligosaccharides released by lichenase treatment of MLG, which releases the characteristic tri- and tetrasaccharides G4G3G and G4G4G3G, respectively, revealed that coleoptile samples in *cslf6* mutants had a 97% decrease of MLG compared to wild type (Table II; Supplemental Fig. S4). This decrease was even more dramatic in seedlings, immature panicles, and mature stems where only traces, if any MLG were detectable in the mutants (Table II; Supplemental Fig. S4). These results were confirmed by measurement of MLG content using a quantitative, but less sensitive, assay specific for MLG, and by immunodot assays using a monoclonal antibody that specifically recognizes MLG epitope (Meikle

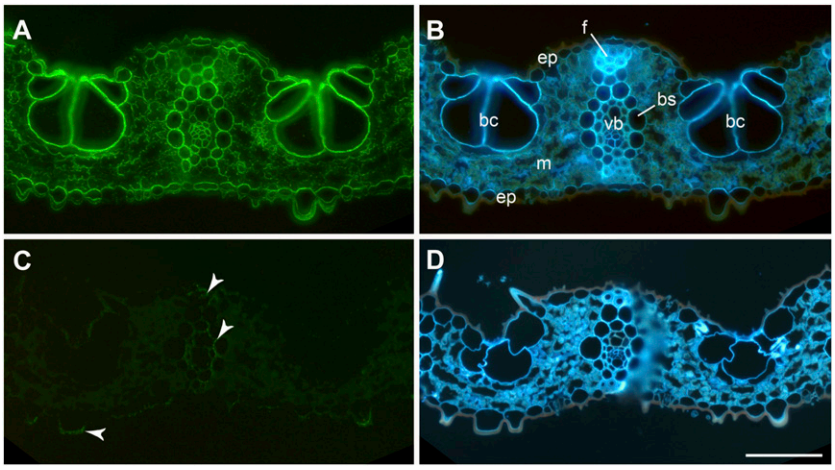

Figure 6. Immunolabeling and staining of fully expanded leaves. Wild type (A) and *cslf6* (C) leaves labeled with anti-MLG monoclonal antibody. Arrowheads in C show weak MLG labeling in sclerenchyma fibers, vascular bundle sheaths, and lower epidermis. B and D show the anatomy wild-type and *cslf6* mutant, respectively, using calcofluor staining. Scale bar: 50 μm; bc, Bulliform cells; bs, bundle sheath; ep, epidermis; f, sclerenchyma fibers; m, mesophyll; vb, vascular bundle.

et al., 1994; Fig. 4; Supplemental Fig. S5). Taken together, these results clearly demonstrate the dramatic decrease in detectable MLG in *cslf6* mutants. As *CslF6* is only one of eight *CslF* genes in rice, we decided to test whether any remaining MLG synthase activity was detectable in the mutants. We measured the endogenous MLG synthase activity in microsomal fractions from 7-d-old seedlings and 4-week-old sheaths of wild-type and mutant plants. We could not detect any residual MLG synthase activity above background levels in the mutant samples (Fig. 2, B and C). We conclude that, with the exception of coleoptiles, the MLG deficiency we observed in the *cslf6* mutant samples is due to a lack of MLG synthase activity and that the other *CslF* family members do not compensate for this loss of enzymatic activity, at least in seedlings and sheaths.

The MLG Deficiency in *cslf6* Mutants Occurs in Both Nonlignified and Lignified Tissues of the Stem But Only in Nonlignified Cells of 3-d-Old Coleoptiles and Leaves

To confirm the results obtained above, immunolabeling using the anti-MLG antibody was carried out on transverse sections of 3-d-old coleoptiles, expanded leaves, and mature stems after grain filling. In the wild-type coleoptiles and developing leaf, MLG occurred in every cell type (Fig. 5A; Supplemental Figs. S6 and S7). In the *cslf6* mutant sections, the MLG detection was severely reduced: Although MLG was still abundant in sclerenchyma cells of the coleoptile and developing leaves, its occurrence was barely visible in the other cell types (Fig. 5B; Supplemental Figs. S6 and S7). To investigate whether this pattern of distribution occurred in developed leaf tissue, we tested the occurrence of MLG epitope in fully expanded leaves of wild type and *cslf6* mutant. In wild-type leaves, the MLG was present in all cell types, including weak labeling in subepidermal sclerenchyma fibers, and was most abundant in the bulliform cells and the cell walls of the vascular bundles and phloem (Fig. 6A). In the *cslf6* mutant, the detection of MLG was low and only observed in a few epidermal and sclerenchyma cells (Fig. 6C). Interestingly, the bulliform cells in expanded leaves of *cslf6* plants showed an aberrant morphology compared to wild type (Fig. 6, B and D). The alteration of MLG occurrence in *cslf6* was even more significant in mature stems. Indeed, MLG was strongly and weakly detected in the parenchyma and sclerenchyma cells, respectively, of wild type (Fig. 5, E and I; Supplemental Fig. S8) whereas no binding was detected in the mutant (Fig. 5, F and J; Supplemental Fig. S8). Interestingly, the absence of MLG in *cslf6* led to opposite patterns of xylan detection in coleoptiles and stems. As shown in Figure 5 and Supplemental Figure S8, the LM10 (xylan) epitope occurrence was higher in the mutant coleoptiles but lower in stems, compared to wild type. This may reflect differences in cell wall architecture that can either be due to distinct polysaccharide interactions inherent to the two organs or distinct reorganization of the cell wall in response to the absence of MLG in *cslf6*. Phloroglucinol staining in coleoptiles and developing leaf (Supplemental Fig. S9) and toluidine blue staining of stems (Fig. 5, K and L) confirmed that sclerenchyma fibers and xylem vessels were lignified in both the wild type and *cslf6* mutant. Previous reports using electron microscopy of immunogold-labeled sections in grass tissues have shown that MLG largely accumulates in the primary cell wall and very little, if any, in secondary cell walls (Trethewey and Harris, 2002; Trethewey et al., 2005). We confirmed that secondary cell walls of wild-type mature stems contain large amount of MLG, while no MLG was present in *cslf6* cell walls, by transmission electron microscopy of immunogold-labeled sections with the anti-MLG antibody (Supplemental Fig. S10). Taken together, these results highlight the major contribution of *CslF6* to MLG biosynthesis in young and mature tissues, and show that *CslF6* function is required for MLG accumulation in secondary cell walls in rice stems.

Mutations in *CslF6* Affect the Mechanical Properties of the Cell Wall

To test whether the MLG deficiency in the *cslf6* mutant affected the mechanical properties of the cell wall, we measured the tensile strength in seedlings and the compression strength in stems, along with their associated strain tolerance parameter. Although we could not detect differences in ultimate strength (force applied per unit of area) between wild-type and mutant seedlings (Supplemental Fig. S11A), cell walls of *cslf6* had significantly lower strain (deformation at breaking) than wild type (Supplemental Fig. S11B). In contrast, for stems, both the cell wall strength and strain properties were significantly reduced in the mutant (Fig. 7). As the strain is a measure of the brittleness of the material, these results show that MLG contributes to the flexibility properties of the cell wall in both seedlings and mature stems, and to cell wall strengthening in stems but not in seedlings.

cslf6 Mutants Have a Significant Reduction in Matrix Polysaccharide Glc Content

We tested whether mutations in *CslF6* cause any changes in cell wall monosaccharide composition. HPAEC analysis of trifluoroacetic-acid-treated samples, which hydrolyzes matrix polysaccharides into monosaccharides (2 M trifluoroacetic acid [TFA] at 121°C for 1 h), revealed that *cslf6* mutants have a severe decrease in Glc content (Table III), which is consistent with the MLG deficiency. These changes were accompanied by significant increases in GalA and moderate decrease in cellulose content in mutant seedlings, and by increases in rhamnose, Gal, GalA, and lignin content in stems of *cslf6* mutants (Tables III and IV).

Mutations in *CslF6* Cause Lesion Mimic Formation, Up-Regulated Defenses, and Enhanced Disease Resistance

After flowering, we observed the appearance of spontaneous, discrete, necrotic lesions in flag and old leaves of the *csfl6* mutant plants (Fig. 8F), suggesting the development of a lesion mimic phenotype. Lesion mimic mutations are characterized by spontaneous lesion formation in plants in the absence of an external stimulus, such as a pathogen (Lorrain et al., 2003). Because many lesion mimic mutations are characterized by enhanced disease resistance and up-regulation of defenses (Lorrain et al., 2003), we tested the response of *cslf6* mutants to bacterial inoculation in leaves. The *cslf6* plants had both decreased lesion size and reduced bacterial growth compared to wild type (Fig. 8, A and B; Supplemental Fig. S12), following inoculation with a virulent isolate of *Xanthomonas oryzae* pv *oryzae*, the causal agent of bacterial blight in rice. To confirm whether the lesion mimic appearance correlates with up-regulated defense responses in the *cslf6* mutants, we tested the expression of three pathogenesis-related (*PR*) genes in intact leaves. *PR* genes are generally induced after pathogen infection or other stresses, and are widely used as markers for cell death and defense responses such as systemic acquired resistance (van Loon et al., 2006). Pathogen and salicylic-acid-responsive genes *PR1a* and *PR1b* (Mitsuhara et al., 2008) as well as the cell-death-related marker gene *PR10* (Kim et al., 2011) were all significantly up-regulated in noninoculated leaves of *cslf6* mutants (Fig. 8, C–E). Interestingly, the same *PR* marker genes were also up-regulated in noninoculated, lesion mimic-free fully expanded leaves of younger plants prior to flowering in *cslf6* mutant plants compared to wild type (Supplemental Fig. S13). These results indicate that loss of MLG activates defense responses and cell death, which correlates with enhanced disease resistance in *cslf6* plants.

DISCUSSION

Previous work has demonstrated that members of the *CslF* and *CslH* subfamilies of glycosyltranferases mediate the biosynthesis of MLG, both in heterologous and native hosts (Burton et al., 2006, 2011; Doblin et al., 2009). *CslF6* is the most widely and highly expressed family member in barley (Burton et al., 2008), *Brachypodium* (Christensen et al., 2010), and rice (Wang et al., 2010). Through functional analysis of *cslf6* loss-of-function mutants, we have shown here that, with the exception of sclerenchyma fibers in coleoptiles, developing leaf, and fully expanded leaves, MLG was undetectable in any other tissues or developmental stages examined, including mature stems. These results demonstrate that the *CslF6* gene has a predominant and nonredundant role in the biosynthesis and accumulation of MLG in nonlignified, primary cell walls of young, expanding tissues in rice, as well as

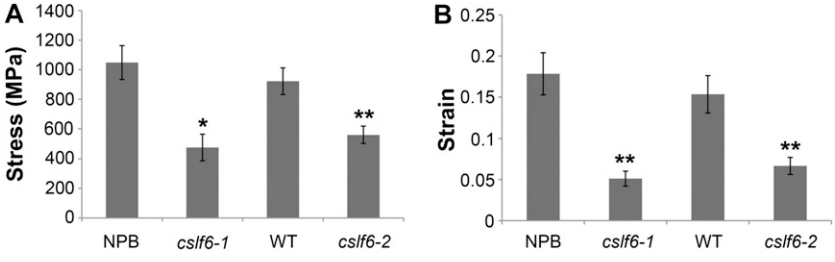

Figure 7. Mechanical properties of cell walls from wild-type and *cslf6* mutant mature stems. A, Stress expressed as compression yield strength (strength at first deformation or bending force). B, Strain (deformation tolerance) as a measure of material brittleness. $n = 12$, ±SD. Significant differences at $P < 0.05$ (*) and $P < 0.001$ (**).

Table III. *Cell wall monosaccharide composition*[a]

Values are average of three replicates ± sd. NPB, Nipponbare wild type; WT, sibling of *cslf6-2* without the insertion. Asterisk (*) indicates statistically significant at $P < 0.05$ and $P < 0.001$ (**).

Sample	Fuc	Rha	Ara	Gal	Glc	Xyl	Man	GalA	GlcA
					μg/mg of AIR				
Seedling									
NPB	2.4 ± 0.3	1.2 ± 0.0	25 ± 2.8	12.4 ± 1.7	34.6 ± 4.4	67.4 ± 5.0	5.7 ± 0.8	8.4 ± 0.8	2.2 ± 0.3
cslf6-1	3.1 ± 0.4	1.5 ± 0.1*	30.2 ± 2.7	15.3 ± 1.1*	7.6 ± 0.7**	69.2 ± 5.9	2.3 ± 0.7*	10.0 ± 0.6*	2.9 ± 0.4*
WT	2.6 ± 0.3	1.2 ± 0.2	24.6 ± 1.4*	12.5 ± 0.9	30.6 ± 1.6	71.6 ± 2.9	3.1 ± 0.7	7.6 ± 0.3	2.2 ± 0.4
cslf6-2	3.1 ± 0.5	1.2 ± 0.2	28.5 ± 1.7	13.7 ± 0.2	7.2 ± 0.2**	73.1 ± 6.5	2.7 ± 0.7	9.9 ± 1.3*	2.8 ± 0.4
Stem									
NPB	0.2 ± 0.0	1.3 ± 0.1	28.6 ± 0.8	10.8 ± 0.6	106.0 ± 9.3	151.6 ± 5.9	0.7 ± 0.02	7.9 ± 0.2	1.5 ± 0.2
cslf6-1	0.3 ± 0.0	1.6 ± 0.0*	33.5 ± 0.4**	12.8 ± 0.6*	49.8 ± 2.2**	179.2 ± 4.1*	0.7 ± 0.03	9.2 ± 0.3*	2.2 ± 0.1*
WT	0.2 ± 0.0	1.3 ± 0.1	31.2 ± 0.7	9.4 ± 0.5	78.5 ± 6.2	161.9 ± 10.1	0.8 ± 0.2	8.4 ± 0.5	1.7 ± 0.4
cslf6-2	0.4 ± 0.0	1.7 ± 0.0*	31.7 ± 0.4	11.5 ± 0.1*	28.3 ± 0.8**	157.8 ± 1.5	1.0 ± 0.1	10.9 ± 0.2**	2.3 ± 0.4

[a]HPAEC analysis after TFA hydrolysis.

being necessary and sufficient for MLG deposition in both nonlignified and lignified tissues in stems. The presence of large amounts of MLG in rice mature stems (after grain filling) is noteworthy, as most other studies in grasses have heavily focused on MLG analysis in coleoptiles, grains, or leaves (Carpita et al., 2001; Gibeaut et al., 2005; Doblin et al., 2009; Christensen et al., 2010; Guillon et al., 2011). Importantly, using electron microscopy, we were able to show that secondary cell walls of sclerenchyma fibers and xylem vessels of rice stems are heavily labeled with anti-MLG epitopes. In a previous study looking at the distribution of MLG in various species representative of the order Poales by electron microscopy, Trethewey et al. (2005) reported that grasses have what they termed type I MLG distribution, with heavy primary cell wall labeling and light secondary cell wall labeling. However, in their study, only leaf samples were labeled for the grass species they selected. It remains to be determined whether other grass species also contain elevated content of MLG in mature stems. However, a preliminary survey revealed very low MLG content in mature stem tissues of switchgrass (*Panicum virgatum*), *Brachypodium*, and maize compared to rice (M.E. Vega-Sánchez, unpublished data), which suggests that the high levels of MLG in mature stems may be unique to rice among the grasses. It is known that *Equisetum arvense*, a nonflowering vascular plant remotely related to the grasses, accumulates a significant amount of MLG in stem cell walls (Sørensen et al., 2008), while species in the Restionaceae and Xyridaceae families in the Poales primarily accumulate MLG in secondary cell walls rather than primary cell walls (Trethewey et al., 2005).

The finding that the other *CslF* family members in rice do not seem to compensate for the loss of *CslF6* function was predicted based on our earlier analysis of large gene families, which addressed putative functional redundancy in gene families by focusing the functional analysis on the most highly expressed family members (Jung et al., 2008). Most of the *CslF* genes are clearly expressed, albeit at much lower levels and in fewer tissue types than *CslF6*, as shown here in Supplemental Figure S1 and in Wang et al. (2010). Whether these genes encode functional proteins needs to be determined, but at least rice *CslF2* and *CslF4* can mediate the biosynthesis of MLG when overexpressed in Arabidopsis, albeit in very small amounts (Burton et al., 2006). It is possible that these genes are involved in the deposition of MLG at stages of development and/or very specific tissue types not represented in our study. In any case, our data strongly suggest that a different gene, other than *CslF6*, is required for deposition of MLG in the sclerenchyma of coleoptiles and leaves. In situ PCR experiments have recently shown that barley *CslH1* expression is restricted to sclerenchyma fiber and xylem cells in leaves (Doblin et al., 2009). Thus, rice *CslH1* is a strong candidate for this function in coleoptiles, developing, and fully expanded leaves as, unlike the other *CslF* genes, *CslH1* and *CslF6* are strongly expressed in coleoptile samples, and *CslH1* is highly expressed in leaves (Supplemental Fig. S1).

Table IV. *Cellulose and lignin content*

ND, Not determined; NPB, Nipponbare wild type; WT, sibling of *cslf6-2* without the insertion. Asterisk (*) indicates statistically significant at $P < 0.05$ and $P < 0.001$ (**).

Sample	Cellulose[a]	Lignin[b]
	μg/mg ± *SD*	
Seedling		
NPB	202.7 ± 6.6	ND
cslf6-1	171.0 ± 16.3*	ND
WT	192.6 ± 32.3	ND
cslf6-2	167.5 ± 9.1	ND
Stem		
NPB	468.3 ± 13.4	131.5 ± 3.7
cslf6-1	461.1 ± 22.0	161.1 ± 15.7*
WT	455.5 ± 11.6	114.4 ± 6.2
cslf6-2	373.7 ± 16.3*	142.4 ± 9.5*

[a]Presented as Glc equivalents of crystalline cellulose. [b]Acetyl bromide lignin.

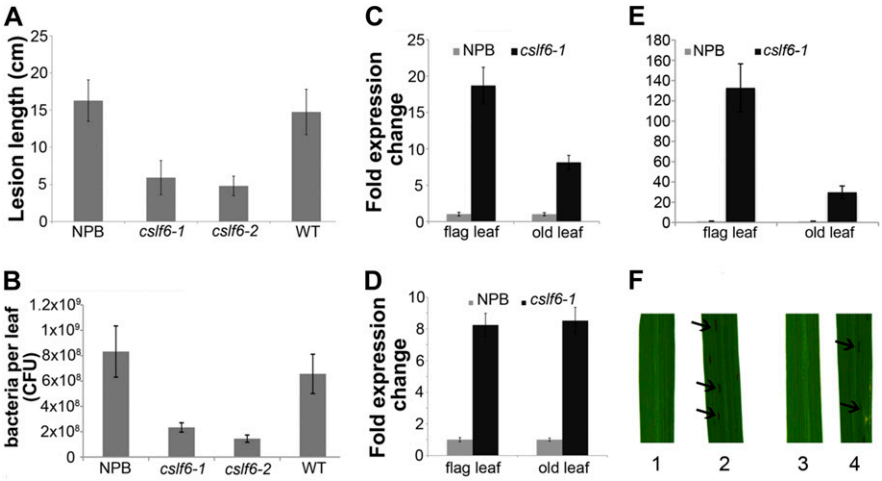

Figure 8. Enhanced disease resistance and up-regulated defenses in *cslf6* mutant. A, Lesion length of rice leaves inoculated with a bacterial suspension of *X. oryzae* pv *oryzae* isolate PXO99. Measurements taken 14 d postinoculation. B, Bacterial titer in PXO99 inoculated leaves, 14 d postinoculation. CFU, Colony forming units; NPB, Nipponbare (wild type); WT, segregant of *cslf6-2* without the insertion. Quantitative reverse transcription-PCR showing the expression of *PR* genes *PR1a* (Os07g03710; C), *PR10* (Os12g36850; D), and *PR1b* (Os01g28450; E) in flag and old leaves of wild-type and mutant plants, prior to inoculation. Values are presented as fold-change expression from the wild type. F, Spontaneous lesion formation on flag leaves of *cslf6* mutants. 1, NPB (WT); 2, *cslf6-1*; 3, WT; 4, *cslf6-2*.

Our results are in agreement with a recent report describing loss-of-function mutations in the barley *CslF6* (*HvCslF6*) gene, which are also known as *beta-glucanless* (*bgl*) mutations (Taketa et al., 2011). Barley *bgl* mutants lack detectable MLG in the endosperm and seedling tissues, including coleoptiles, and in mature leaves (Tonooka et al., 2009; Taketa et al., 2011). The lack of detectable MLG in barley coleoptiles suggests that *HvCslF6* may be required for MLG deposition in sclerenchyma fibers in this tissue, in contrast to rice. However, the *bgl* seedling tissues including the coleoptiles, were also considerably older than the rice coleoptiles analyzed here (10 d versus 3 d) and it is possible that if there was any MLG in the *bgl* coleoptiles it may have been degraded since it is known that the MLG content of coleoptiles declines after elongation (Gibeaut et al., 2005). Analysis of younger *bgl* tissues and immunolabeling studies are needed to confirm this. Nevertheless, it is clear that the *CslF6* gene has a unique and nonredundant role in MLG biosynthesis in both rice and barley, and likely in other grasses as well, such as wheat (Nemeth et al., 2010).

In this study, we used several independent methods to confirm the deficiency of MLG in the *clsf6* mutants. One explanation for the trace levels of MLG in *cslf6* mutants could be enhanced degradation by the activity of the (1,3; 1,4)-β-D-glucan endohydrolases, which are believed to hydrolyze MLG in growing tissues (Inouhe and Nevins, 1991). Although we cannot completely rule out this possibility, we hypothesize that the lack of MLG in the mutants is primarily due to a loss of synthase activity, as is clearly shown in our endogenous MLG synthase activity assays in seedlings and sheaths (Fig. 2, B and C). Moreover, the presence of high amounts of MLG in wild-type mature stem samples, a tissue no longer expanding, coupled to the low expression levels of *CslF6* in these tissues (Fig. 1B), suggests that MLG is deposited in stems prior to maturity and is not hydrolyzed by (1,3; 1,4)-β-D-glucan endohydrolases. The fact that *CslF6* is expressed in young stems (tillers in Fig. 1B) and MLG synthase activity is detectable at this stage in wild-type plants (Fig. 2C), but not in mature stems (U. Christensen and M.E. Vega-Sánchez, unpublished data), is in agreement with this hypothesis.

The role of the primary cell wall in the control of cell expansion has been largely documented, and various models exist that describe the arrangement of cellulose microfibrils among a matrix or network of cross-linking hemicellulosic polysaccharides (Cosgrove, 2001, 2005). In grass vegetative tissues, MLG has been implicated in the regulation of cell expansion (Carpita, 1996; Gibeaut et al., 2005; Christensen et al., 2010) and two complementary models of its association with cellulose microfibrils have been suggested: one where MLG primarily coats the cellulose microfibrils while arabinoxylans serve as the cross-linking units (Carpita et al., 2001), and another in which MLG primarily forms a gel-like matrix around the microfibrils with occasional formation of junction zones with cellulose and other polysaccharides (Fincher, 2009a, 2009b). Thompson has argued that polysaccharides forming these cross-links or tethers between microfibrils will share the main load-bearing functions of the cell wall with cellulose (Thompson, 2005), and this suggests that plants with deficiencies in these polysaccharides should show similar severe growth and developmental phenotypes

as primary cell wall cellulose synthase (*cesa*) mutants (Arioli et al., 1998; Persson et al., 2007). The dramatic reduction of MLG (>99% in most tissues), accompanied by an absence of major growth and developmental defects in *cslf6* mutants suggests that MLG does not act as a major load-bearing component of the primary cell wall in rice and thus may not participate as a cross-linking polysaccharide. These observations are supported by the tensile strength results that suggest that MLG acts more like a gel matrix that provides flexibility meanwhile strengthening the cell wall in growing tissues such as seedlings, in agreement with a model proposed by Fincher (Fincher, 2009a, 2009b). We found that mutant seedlings had a moderate decrease in cellulose content (Table IV), which can also explain the reduced resistance to deformation in *cslf6* plants. In addition, our data suggests that MLG plays a role in cell elongation, but less predominantly so than would have been expected for a polysaccharide strongly associated with growing tissues. The reduction in cell elongation in coleoptiles was moderate (28%–30%) and is in agreement with the 33% height difference in fully developed plants. One possibility for MLG's transient accumulation in growing tissues is that it serves as an energy source, especially in conditions of sugar depletion, as shown in wheat leaves (Roulin and Feller, 2001; Fincher, 2009a). In contrast, we found that in nongrowing tissues, such as mature stems, the distribution of MLG in vascular bundles and sclerenchyma fibers is in agreement with a role in cell wall reinforcement, which was supported by the compression test results that revealed a weaker and more brittle cell wall in the *cslf6* mutant. It is interesting to note that the lack of MLG in stems is accompanied by increases in lignin, rhamnose, Gal, and GalA content (Table III). These likely reflect cell wall changes that compensate for the lack of MLG. Mutants with mild developmental phenotypes and lacking detectable levels of xyloglucan (Cavalier et al., 2008) and stem glucomannan (Goubet et al., 2009) have been recently characterized in Arabidopsis. These and our results with rice *cslf6* mutants suggest that the plant can adapt and compensate, to a certain extent, for losses in major hemicellulosic polysaccharides in the cell wall. Taken together, our results add to a growing number of observations suggesting that current models of cross-linking of cellulose microfibrils as a fundamental principle to ensure cell wall integrity need revision (Scheller and Ulvskov, 2010).

The discovery of lesion formation and up-regulated defenses leading to enhanced disease resistance in the *cslf6* mutant adds to the growing number of cell wall mutations that have broad effects on cellular homeostasis beyond the well-characterized mechanical stress support functions typically associated with plant cell walls (Pilling and Höfte, 2003; Cantu et al., 2008; Seifert and Blaukopf, 2010). For example, mutations in the Arabidopsis *MUR3* (*MURUS3*) gene, which is involved in xyloglucan biosynthesis, also cause lesion formation, up-regulated defense gene expression, and enhanced resistance to a downy mildew pathogen (Tedman-Jones et al., 2008). It has been widely documented that plants can sense and monitor disturbances or changes in cell wall integrity and activate signaling pathways in response to these wall feedback stimuli (Pilling and Höfte, 2003; Bart et al., 2010; Seifert and Blaukopf, 2010). Our data suggests that the absence of MLG in the cell wall triggers a signaling cascade that activates stress and defense-related gene expression, and eventually, a cell death program. This is supported by the finding that PR marker genes are up-regulated in younger leaves even in the absence of lesion mimics, which suggest that *cslf6* plants are primed for the onset of cell death at later stages of development. For this reason, we believe that the enhanced resistance phenotype we observed in *cslf6* plants is a consequence of such a program. The actual mechanism that activates these defenses in *cslf6* remains to be elucidated. It is possible that MLG oligosaccharides can function as signaling molecules to repress defense responses in wild-type plants, analogous to bacterial cyclic β-(1,2)-glucans that have been shown to suppress the plant's defense response (Rigano et al., 2007).

In summary, we have shown that *CslF6* is required for MLG accumulation in nonlignified, primary cell walls of rice, and necessary and sufficient for MLG deposition in lignified, secondary cell walls of mature stems but not coleoptiles, developing, and fully expanded leaves. Our results demonstrate the importance of MLG in maintaining the mechanical properties of the cell wall, as well as highlight how the plant can adapt and rearrange its cell wall environment to compensate for the lack of this polysaccharide. The absence of gross morphological phenotypes observed in plants with low or no content of xyloglucan (Cavalier et al., 2008), glucomannan (Goubet et al., 2009), or, as shown here, MLG, underscores the necessity to redefine current models of cell wall architecture.

MATERIALS AND METHODS

Plant Material and Growth Conditions

Rice (*Oryza sativa*) was grown in growth chambers with the following conditions: 12 h daylight, 470 μmol m^{-2} s^{-1} illumination intensity, 80% relative humidity, 26°C for 1 h at the beginning and end of the cycle, and 28°C for the remaining 10 h; 12 h dark, 80% relative humidity, 26°C. Transposon insertion lines in the Nipponbare cultivar background were obtained from the Commonwealth Scientific and Industrial Research Organization collection in Australia and homozygous lines for each independent insertion were identified by PCR. The generation of the transposon insertion lines is described in Upadhyaya et al. (2006).

Preparation of AIR and MLG Oligosaccharide Fingerprinting

Samples were collected from various rice organs or infiltrated *Nicotiana benthamiana* leaves, frozen in liquid nitrogen, and freeze dried overnight using a lyophilizer. AIR preparation and destarching was done according to methods described in Harholt et al. (2006). For the detection of MLG oligosaccharides, AIR (5 mg) was sequentially extracted as follows: 0.05 M

1,2-cyclohexylenedi nitrilo-tetraacetic acid (pH 6.5) for 24 h at room temperature (RT); 0.05 M Na_2CO_3 containing 0.01 M $NaBH_4$ for 24 h; and then with 4 M KOH containing 0.01 M $NaBH_4$ for 24 h at RT (4 M KOH fraction). The pH of the 4 M KOH fraction was adjusted to pH 5 with glacial acetic acid, dialyzed against deionized water, and then lyophilized. The KOH fraction was digested with 0.5 units lichenase (from *Bacillus subtilis*, Megazyme) in 0.02 M sodium phosphate buffer (pH 6.5) at 50°C with continuous mixing for 24 h. The reaction was stopped by boiling at 100°C for 2 min, cooled to ambient temperature, and centrifuged prior to HPAEC analysis. The released oligosaccharides after enzymatic digestion were separated by HPAEC on a Dionex DX600 system equipped with a pulsed amperometric detector. A CarboPac PA200 column (3 × 250 mm) eluted with a gradient of 0 to 250 mM sodium acetate in 100 mM NaOH over 40 min at 0.4 mL/min was used. G4G4G3G, G4G3G (Megazyme), and cellodextrins (Sigma-Aldrich) were run as standards.

Quantitative Reverse-Transcriptase PCR

Total RNA was extracted using the RNeasy plant mini kit (Qiagen) following manufacturer's instructions. RNA preparations were treated with DNase1 (Sigma-Aldrich) to remove traces of DNA contamination. One microgram of RNA was used for reverse transcription with the Transcriptor high fidelity cDNA synthesis kit (Roche) and oligo dT primers. After synthesis, the cDNA reaction was diluted three times in ultrapure water, and 1 μL was used for PCR using the Fast SYBR Green master mix (Applied Biosystems) and gene-specific primers (Supplemental Table S1) in a StepONE plus Q-PCR machine (Applied Biosystems).

Plasmids and Constructs

Full-length cDNA clones for *CslF6* (AK065259.1) and *CslA1* (OsJNEa07E18) were identified and ordered from the Knowledge-Based *Oryza* Molecular Biological Encyclopedia (http://cdna01.dna.affrc.go.jp/cDNA/) and the AZ Genomics Institute (http://www2.genome.arizona.edu/) collections, respectively. The cDNA for *CslA6* was amplified by PCR using gene-specific primers (Supplemental Table S1) from first-strand cDNA made from pooled rice samples. Entry clones for cloning using the Gateway technology (Invitrogen) were made by amplifying the coding sequences for each gene using Gateway-compatible primers (Supplemental Table S1), as follows: PCR reactions were gel purified using the MinElute gel extraction kit (Qiagen) and used for BP recombination reactions into pDONR-Zeocin (Invitrogen) for *CslF6* and *CslA1*, and pENTR-D-TOPO cloning (Invitrogen) for *CslA6*, following manufacturer's instructions. Entry clones were finally used for Gateway recombination into the destination vector pEarleyGate 201 (Earley et al., 2006) using LR clonase enzyme mix (Invitrogen).

Infiltration of *Agrobacterium tumefasciens* into *N. benthamiana*

Infiltration of leaves of 4-week-old *N. benthamiana* plants was done using *A. tumefasciens* strain C58 (OD = 1), following the method described in Jensen et al. (2008). AIR preparations and MLG content measurements were done on leaves 5 d postinfiltration, as described below. The *CslA1* and *CslA6* constructs were infiltrated as negative controls to show that only *CslF6* mediates the biosynthesis of MLG in this heterologous host *(CslA1*, *CslA6*, and *CslF6* all belong to the same GT2 family of glycosyltranferases).

MLG Content Determination

For MLG content measurement, the mixed-linkage β-glucan assay from Megazyme was used, adapting the manufacturer's instructions for small-scale (5 mg AIR) preparations in microtubes by dividing all reaction volumes by 10. In this assay, cell walls are digested with lichenase, a (1,3; 1,4)-β-D-glucan endohydrolase, which releases specific oligosaccharides that are then digested to Glc by β-glucosidase treatment. The Glc is then quantified colorimetrically by a reaction involving Glc oxidase and peroxidase.

Determination of (1,3; 1,4)-β-D-Glucan Synthase Activity

Microsomes were extracted as described in Christensen and Scheller (2012) with slight modifications using approximately 0.5 g (fresh weight) of tissue. A reaction mixture consisting of 100 μg microsome protein, 0.2 mM UDP-Glc (Sigma-Aldrich), 0.56 kBq UDP-^{14}C-Glc (ARC), 20 mM $MgCl_2$, 200 mM Suc, 50 mM Tris-HCl pH 8.5 in a total volume of 50 μL was incubated at 25°C with agitation for 1 h. The product was subsequently precipitated and detected according to Christensen and Scheller (2012).

Preparation of Plant Material for Microscopy

Three-day-old coleoptiles, fully expanded leaves, and mature second stem internode pieces were fixed for 24 h at 4°C in 4% paraformaldehyde in 50 mM piperazine-N,N′-bis(2-ethanesulphonic acid), 5 mM EGTA, 5 mM MgSO4, pH 6.9 as described in Verhertbruggen et al. (2009). The coleoptile pieces were cut from the basal region of the organ and were 4.0- and 6.0-mm long for longitudinal and transverse sections, respectively. Stem sections (1 cm long) were 2-cm distal from the second node with the first internode being the youngest internode (from the top). Coleoptiles were embedded in 7% agarose and sectioned (60 μm) using a Leica VT1000S vibratome as described in Manabe et al. (2011). For cell length and diameter measurement, the coleoptile sections were analyzed under light microscopy. Cell measurements were done using Metamorph software calibrated with a 1-mm micrometer certified by National Physical Laboratory. Fully expanded leaves and mature second stem internode were embedded in LR white resin as described in Yin et al. (2011). Stems and leaves were washed once in distilled water for 10 min, dehydrated at RT by incubation in a gradient of aqueous alcohol (10%, 20%, and 30% [v/v] ethanol [10 min for each solution], 50%, 70%, 90%, and 100% [v/v] ethanol [30 min for each solution], and overnight in 100% [v/v] ethanol) and infiltrated with LR white resin by incubation in a gradient of LR White/ethanol solution (10%, 20%, 30%, 50%, 70%, and 90% [v/v] resin [60 min for each solution, RT] and three times 100% [v/v] resin [overnight, 8 h, overnight at 4°C]). After polymerization at 65°C for 5 d, LR white embedded fully expanded leaves and stem internodes were sectioned (2 and 0.5 μm thick, respectively) with an ultramicrotome and disposed on 10-well slides coated with Vectabond.

Immunofluorescence Microscopy

For each genotype, over 50 transverse sections from 12 coleoptiles, 12 transverse sections from two stems, and 12 sections from two leaves were immunolabeled and analyzed as described in Verhertbruggen et al. (2009). Rice material was incubated for 30 min at RT in a 5% milk powder protein/phosphate-buffered saline (PBS) solution, extensively washed with PBS, and incubated for 90 min at RT with primary monoclonal antibodies (10-fold dilution rat antixylan LM10 [McCartney et al., 2005] or 1,000-fold mouse anti-MLG [Meikle et al., 1994]). The antixylan LM10 was first used to demonstrate that polysaccharides other than MLG could be detected in cslf6 plants. After extensive washes in PBS, the sections were incubated for 90 min at RT in the darkness with anti-rat or anti-mouse monoclonal antibodies coupled with fluorescein isothiocyanate. Secondary monoclonal antibodies were diluted 100-fold in 5% milk powder protein/PBS solution. After incubation with secondary antibody, the samples were washed in PBS, incubated at RT for 1 min in the darkness with 0.1 M Calcofluor, washed again in PBS, and mounted on slides with Citifluor AF1. Immunofluorescence detected in stems and coleoptiles was captured with a Q-imaging camera mounted on a Leica DM4000B epifluorescence microscope. Fully expanded leaves were visualized with a Zeiss Axioimager M1 compound microscope; fluorescein isothiocyanate antibody label was detected using blue excitation and a GFP narrow-band emission filter, and calcofluor staining was observed in the same section with UV excitation and a long pass emission filter. Sections incubated without primary antibody were used as negative control and are shown in Supplemental Figures S7 and S8, labeling of wild type or with LM10 are positive controls. Immunolabeling was done at least in triplicate. Wild-type and mutant micrographs were captured and processed in Adobe Photoshop CS4 with the exact same values.

Bacterial Inoculation

Inoculation of rice leaves with *Xanthomonas oryzae* pv *oryzae* isolate PXO99, lesion size measurement, and bacterial titer determination were carried out as described in Bart et al. (2010).

Tensile Strength Assay

Ultimate stress and strain were measured using an in-house tensile testing instrument, which consists of a stepper motor and a sensitive load cell. The

stepper motor was calibrated every day, prior to measurements, with an in-line screw gauge. The force sensor, as suggested by the manufacturer, was calibrated with known quantities of water from 0 to 1,500*g* force (0, 250, 500, 750, 1,000, and 1,500 gf were used as calibration points; 1 N = 101.97 gf). Further, rectangular strips of Whatman glass microfiber filters were subjected to tensile tests and the resulting stress and strain values had SDs of less than 5%. Six-day-old seedlings were used. The diameter of the seedling near its base and its total length were measured. The seedlings were then glued on to the sample holders using hot glue (Stanley DualMelt). Only 5 mm of the culm remained unglued between the sample holders. The sample holders were then screwed on to the apparatus and the tensile strength measurements were taken at RT. The sample holders consisted of a support system for the unglued portion of the culm to prevent it from damage during the holder installation. The support was removed from the holder just before starting the analysis. The stepper motor (IMC17-S04-A, RMS motion) was used to maintain a constant speed rate of 50 μm/s. The force sensor (ADW 15, LCM systems) was used to measure the force applied by the motor on the seedling. The instrument was digitally controlled and data were also collected digitally. The constant speed rate was used to calculate the elongation of the culm as a product of strain rate and time elapsed. Strain was then calculated as a ratio of elongation to the length of the suspended culm (5 mm). Stress was calculated as a ratio of the force and cross-sectional area of the culm. The ultimate stress and the corresponding strain at the breaking point were established from a stress versus strain plot (Supplemental Fig. S14). The ultimate stress represents the maximum load a material can take before failure and the strain corresponding to ultimate stress represents a measure of the brittle/ductile nature of the material. Materials with low strain are characterized as brittle. For the stem strength assay, mature (after grain filling) floral bolt stems from 4-month-old plants were subjected to compression tests. Compression strength was measured on the same instrument but the motor was driven in the opposite direction to tensile testing. The compression yield strength, based on the first deformation of the stem, and the corresponding strain were recorded from the stress-strain graph. Representative stress versus strain plots are shown in Supplemental Figure S14.

Monosaccharide Composition Analysis

Cell wall monosaccharide composition following TFA hydrolysis (2 M TFA at 121°C for 1 h) was determined from AIR samples of 7-d-old seedlings and mature second internode stems using HPAEC according to methods described in ØBro et al. (2004). For the separation of Xyl and Man peaks, samples were run on a CarboPac SA10 column (Dionex) with 1 mM KOH eluent over 11 min at a flow rate of 1 mL/min, using a Dionex ICS3000 unit equipped with a pulse amperometric detector.

Acetyl Bromide Lignin Determination

Lignin content was estimated from AIR samples using the method from Fukushima and Hatfield (2001). The extinction coefficient used for rice samples was 17.75.

Cellulose Content Determination

For the determination of cellulose content, AIR samples were first treated with TFA (2 M TFA at 121°C for 1 h) to remove matrix polysaccharides and then treated with 72% (w/w) sulphuric acid at 120°C as described in Bart et al. (2010). Cellulose was estimated as Glc equivalents from the sulphuric acid hydrolysates using HPAEC.

Sequence data from this article can be found in the GenBank/EMBL data libraries under accession numbers NM_001067583 (*CslF6*).

Supplemental Data

The following materials are available in the online version of this article.

Supplemental Figure S1. Digital expression analysis of *CslF* genes in rice.

Supplemental Figure S2. *CslF6* gene structure and identification of knockout lines.

Supplemental Figure S3. *cslf6* mutant flower phenotypes.

Supplemental Figure S4. HPAEC analysis of oligosaccharides released from MLG by digestion with lichenase.

Supplemental Figure S5. Immunodot assays showing MLG content in different tissues.

Supplemental Figure S6. Indirect immunodetection of transverse sections through the coleoptile and developing leaf.

Supplemental Figure S7. Immunolabeling of coleoptiles sections.

Supplemental Figure S8. Immunolabeling of stem internode sections.

Supplemental Figure S9. Pholoroglucinol-HCl staining of 3-d-old coleoptile and developing leaf sections of wild-type (NPB) and *cslf6-1* mutant.

Supplemental Figure S10. Transmission electron micrographs of mature stem sections immunogold labeled for the anti-MLG antibody.

Supplemental Figure S11. Mechanical properties of cell walls of *cslf6* and wild-type seedlings.

Supplemental Figure S12. Lesion length on rice plants inoculated with *X. oryzae pv oryzae* isolate PXO99.

Supplemental Figure S13. Up-regulated defenses in *cslf6* mutant plants prior to flowering stage.

Supplemental Figure S14. In-house tensile strength testing instrument and representative stress versus strain plots.

Supplemental Table S1. List of primers used in this study.

ACKNOWLEDGMENTS

We would like to thank Dr. Narayana Upadhyaya for providing seeds of *cslf6* insertion mutants; Jeemeng Lao and Jacob Katsnelson for technical assistance; Sherry Chan for plant growth and care; Lina Prak for assistance with LR white embedding and microtome sectioning of rice stems; and Drs. Brad Holmes and Berit Ebert for help with HPAEC protocols and equipment setup.

Received February 10, 2012; accepted February 29, 2012; published March 2, 2012.

LITERATURE CITED

Arioli T, Peng L, Betzner AS, Burn J, Wittke W, Herth W, Camilleri C, Höfte H, Plazinski J, Birch R, et al (1998) Molecular analysis of cellulose biosynthesis in *Arabidopsis.* Science **279:** 717–720

Bart RS, Chern M, Vega-Sánchez ME, Canlas P, Ronald PC (2010) Rice *Snl6*, a cinnamoyl-CoA reductase-like gene family member, is required for NH1-mediated immunity to *Xanthomonas oryzae* pv. *oryzae*. PLoS Genet **6:** e1001123

Burton RA, Collins HM, Kibble NAJ, Smith JA, Shirley NJ, Jobling SA, Henderson M, Singh RR, Pettolino FA, Wilson SM, et al (2011) Over-expression of specific HvCslF cellulose synthase-like genes in transgenic barley increases the levels of cell wall (1,3;1,4)-β-d-glucans and alters their fine structure. Plant Biotechnol J **9:** 117–135

Burton RA, Fincher GB (2009) (1,3;1,4)-Beta-D-glucans in cell walls of the poaceae, lower plants, and fungi: a tale of two linkages. Mol Plant **2:** 873–882

Burton RA, Jobling SA, Harvey AJ, Shirley NJ, Mather DE, Bacic A, Fincher GB (2008) The genetics and transcriptional profiles of the cellulose synthase-like *HvCslF* gene family in barley. Plant Physiol **146:** 1821–1833

Burton RA, Wilson SM, Hrmova M, Harvey AJ, Shirley NJ, Medhurst A, Stone BA, Newbigin EJ, Bacic A, Fincher GB (2006) Cellulose synthase-like *CslF* genes mediate the synthesis of cell wall (1,3;1,4)-beta-D-glucans. Science **311:** 1940–1942

Cantu D, Vicente AR, Labavitch JM, Bennett AB, Powell AL (2008) Strangers in the matrix: plant cell walls and pathogen susceptibility. Trends Plant Sci **13:** 610–617

Cao PJ, Bartley LE, Jung KH, Ronald PC (2008) Construction of a rice glycosyltransferase phylogenomic database and identification of rice-diverged glycosyltransferases. Mol Plant **1:** 858–877

Carpita NC (1996) Structure and biogenesis of the cell walls of grasses. Annu Rev Plant Physiol Plant Mol Biol **47:** 445–476

Carpita NC, Defernez M, Findlay K, Wells B, Shoue DA, Catchpole G, Wilson RH, McCann MC (2001) Cell wall architecture of the elongating maize coleoptile. Plant Physiol **127:** 551–565

Cavalier DM, Lerouxel O, Neumetzler L, Yamauchi K, Reinecke A, Freshour G, Zabotina OA, Hahn MG, Burgert I, Pauly M, et al (2008) Disrupting two *Arabidopsis thaliana* xylosyltransferase genes results in plants deficient in xyloglucan, a major primary cell wall component. Plant Cell **20:** 1519–1537

Chen L, Kamisaka S, Hoson T (1999) Suppression of (1->3),(1->4)-beta-D-glucan during light-induced inhibition of rice coleoptile growth. J Plant Res **112:** 7–13

Christensen U, Alonso-Simon A, Scheller HV, Willats WG, Harholt J (2010) Characterization of the primary cell walls of seedlings of *Brachypodium distachyon*—a potential model plant for temperate grasses. Phytochemistry **71:** 62–69

Christensen U, Scheller HV (2012) Regulation of (1,3;1,4)-β-D-glucan synthesis in developing endosperm of barley *lys* mutants. J Cereal Sci **55:** 69–76

Cosgrove DJ (2001) Wall structure and wall loosening: a look backwards and forwards. Plant Physiol **125:** 131–134

Cosgrove DJ (2005) Growth of the plant cell wall. Nat Rev Mol Cell Biol **6:** 850–861

Demirbas A (2005) Beta-glucan and mineral nutrient contents of cereals grown in Turkey. Food Chem **90:** 773–777

Doblin MS, Pettolino FA, Wilson SM, Campbell R, Burton RA, Fincher GB, Newbigin E, Bacic A (2009) A barley cellulose synthase-like *CSLH* gene mediates (1,3;1,4)-beta-D-glucan synthesis in transgenic *Arabidopsis*. Proc Natl Acad Sci USA **106:** 5996–6001

Earley KW, Haag JR, Pontes O, Opper K, Juehne T, Song K, Pikaard CS (2006) Gateway-compatible vectors for plant functional genomics and proteomics. Plant J **45:** 616–629

Fincher GB (2009a) Exploring the evolution of (1,3;1,4)-beta-D-glucans in plant cell walls: comparative genomics can help! Curr Opin Plant Biol **12:** 140–147

Fincher GB (2009b) Revolutionary times in our understanding of cell wall biosynthesis and remodeling in the grasses. Plant Physiol **149:** 27–37

Fry SC, Nesselrode BHWA, Miller JG, Mewburn BR (2008) Mixed-linkage (1,3; 1,4)-beta-D-glucan is a major hemicellulose of Equisetum (horsetail) cell walls. New Phytol **179:** 104–115

Fukushima RS, Hatfield RD (2001) Extraction and isolation of lignin for utilization as a standard to determine lignin concentration using the acetyl bromide spectrophotometric method. J Agric Food Chem **49:** 3133–3139

Gibeaut DM, Pauly M, Bacic A, Fincher GB (2005) Changes in cell wall polysaccharides in developing barley (*Hordeum vulgare*) coleoptiles. Planta **221:** 729–738

Goubet F, Barton CJ, Mortimer JC, Yu X, Zhang Z, Miles GP, Richens J, Liepman AH, Seffen K, Dupree P (2009) Cell wall glucomannan in *Arabidopsis* is synthesised by CSLA glycosyltransferases, and influences the progression of embryogenesis. Plant J **60:** 527–538

Guillon F, Bouchet B, Jamme F, Robert P, Quéméner B, Barron C, Larré C, Dumas P, Saulnier L (2011) *Brachypodium distachyon* grain: characterization of endosperm cell walls. J Exp Bot **62:** 1001–1015

Harholt J, Jensen JK, Sørensen SO, Orfila C, Pauly M, Scheller HV (2006) ARABINAN DEFICIENT 1 is a putative arabinosyltransferase involved in biosynthesis of pectic arabinan in Arabidopsis. Plant Physiol **140:** 49–58

Hazen SP, Scott-Craig JS, Walton JD (2002) Cellulose synthase-like genes of rice. Plant Physiol **128:** 336–340

Honegger R, Haisch A (2001) Immunocytochemical location of the (1,3)(1,4)-beta-glucan lichenin in the lichen-forming ascomycete *Cetraria islandica* (Icelandic moss). New Phytol **150:** 739–746

Inouhe M, Nevins DJ (1991) Inhibition of auxin-induced cell elongation of maize coleoptiles by antibodies specific for cell wall glucanases. Plant Physiol **96:** 426–431

Jensen JK, Sørensen SO, Harholt J, Geshi N, Sakuragi Y, Møller I, Zandleven J, Bernal AJ, Jensen NB, Sørensen C, et al (2008) Identification of a xylogalacturonan xylosyltransferase involved in pectin biosynthesis in *Arabidopsis*. Plant Cell **20:** 1289–1302

Jung KH, Dardick C, Bartley LE, Cao P, Phetsom J, Canlas P, Seo YS, Shultz M, Ouyang S, Yuan Q, et al (2008) Refinement of light-responsive transcript lists using rice oligonucleotide arrays: evaluation of gene-redundancy. PLoS ONE **3:** e3337

Kim SG, Kim ST, Wang Y, Yu S, Choi IS, Kim YC, Kim WT, Agrawal GK, Rakwal R, Kang KY (2011) The RNase activity of rice probenazole-induced protein1 (PBZ1) plays a key role in cell death in plants. Mol Cells **31:** 25–31

Kimpara T, Aohara T, Soga K, Wakabayashi K, Hoson T, Tsumuraya Y, Kotake T (2008) Beta-1,3:1,4-glucan synthase activity in rice seedlings under water. Ann Bot (Lond) **102:** 221–226

Lorrain S, Vailleau F, Balagué C, Roby D (2003) Lesion mimic mutants: keys for deciphering cell death and defense pathways in plants? Trends Plant Sci **8:** 263–271

Manabe Y, Nafisi M, Verhertbruggen Y, Orfila C, Gille S, Rautengarten C, Cherk C, Marcus SE, Somerville S, Pauly M, et al (2011) Loss-of-function mutation of *REDUCED WALL ACETYLATION2* in Arabidopsis leads to reduced cell wall acetylation and increased resistance to *Botrytis cinerea*. Plant Physiol **155:** 1068–1078

McCartney L, Marcus SE, Knox JP (2005) Monoclonal antibodies to plant cell wall xylans and arabinoxylans. J Histochem Cytochem **53:** 543–546

Meikle PJ, Hoogenraad NJ, Bonig I, Clarke AE, Stone BA (1994) A (1—>3,1—>4)-beta-glucan-specific monoclonal antibody and its use in the quantitation and immunocytochemical location of (1—>3,1—>4)-beta-glucans. Plant J **5:** 1–9

Mitsuhara I, Iwai T, Seo S, Yanagawa Y, Kawahigasi H, Hirose S, Ohkawa Y, Ohashi Y (2008) Characteristic expression of twelve rice *PR1* family genes in response to pathogen infection, wounding, and defense-related signal compounds (121/180). Mol Genet Genomics **279:** 415–427

Nemeth C, Freeman J, Jones HD, Sparks C, Pellny TK, Wilkinson MD, Dunwell J, Andersson AA, Aman P, Guillon F, et al (2010) Down-regulation of the *CSLF6* gene results in decreased (1,3;1,4)-beta-D-glucan in endosperm of wheat. Plant Physiol **152:** 1209–1218

ØBro J, Harholt J, Scheller HV, Orfila C (2004) Rhamnogalacturonan I in *Solanum tuberosum* tubers contains complex arabinogalactan structures. Phytochemistry **65:** 1429–1438

Persson S, Paredez A, Carroll A, Palsdottir H, Doblin M, Poindexter P, Khitrov N, Auer M, Somerville CR (2007) Genetic evidence for three unique components in primary cell-wall cellulose synthase complexes in *Arabidopsis*. Proc Natl Acad Sci USA **104:** 15566–15571

Pettolino FA, Sasaki I, Turbic A, Wilson SM, Bacic A, Hrmova M, Fincher GB (2009) Hyphal cell walls from the plant pathogen Rhynchosporium secalis contain (1,3/1,6)-beta-D-glucans, galacto- and rhamnomannans, (1,3;1,4)-beta-D-glucans and chitin. FEBS J **276:** 3698–3709

Pilling E, Höfte H (2003) Feedback from the wall. Curr Opin Plant Biol **6:** 611–616

Popper ZA, Fry SC (2003) Primary cell wall composition of bryophytes and charophytes. Ann Bot (Lond) **91:** 1–12

Rigano LA, Payette C, Brouillard G, Marano MR, Abramowicz L, Torres PS, Yun M, Castagnaro AP, Oirdi ME, Dufour V, et al (2007) Bacterial cyclic beta-(1,2)-glucan acts in systemic suppression of plant immune responses. Plant Cell **19:** 2077–2089

Roulin S, Feller U (2001) Reversible accumulation of (1—>3,1—>4)-beta-glucan endohydrolase in wheat leaves under sugar depletion. J Exp Bot **52:** 2323–2332

Scheller HV, Ulvskov P (2010) Hemicelluloses. Annu Rev Plant Biol **61:** 263–289

Seifert GJ, Blaukopf C (2010) Irritable walls: the plant extracellular matrix and signaling. Plant Physiol **153:** 467–478

Shibuya N, Nakane R, Yasui A, Tanaka K, Iwasaki T (1985) Comparative studies on cell wall preparations from rice bran, germ, and endosperm. Cereal Chemistry **62:** 252–258

Smith BG, Harris PJ (1999) The polysaccharide composition of Poales cell walls: Poaceae cell walls are not unique. Biochem Syst Ecol **27:** 33–53

Sørensen I, Pettolino FA, Wilson SM, Doblin MS, Johansen B, Bacic A, Willats WG (2008) Mixed-linkage (1→3),(1→4)-beta-D-glucan is not unique to the Poales and is an abundant component of Equisetum arvense cell walls. Plant J **54:** 510–521

Taketa S, Yuo T, Tonooka T, Tsumuraya Y, Inagaki Y, Haruyama N, Larroque O, Jobling SA (2012) Functional characterization of barley betaglucanless mutants demonstrates a unique role for CslF6 in (1,3;1,4)-{beta}-D-glucan biosynthesis. J Exp Bot **63:** 381–392

Tedman-Jones JD, Lei R, Jay F, Fabro G, Li X, Reiter WD, Brearley C, Jones JD (2008) Characterization of *Arabidopsis mur3* mutations that result in constitutive activation of defence in petioles, but not leaves. Plant J **56:** 691–703

Thompson DS (2005) How do cell walls regulate plant growth? J Exp Bot **56:** 2275–2285

Tonooka T, Aoki E, Yoshioka T, Taketa S (2009) A novel mutant gene for (1-3, 1-4)-beta-D-glucanless grain on barley (*Hordeum vulgare* L.) chromosome 7H. Breed Sci **59:** 47–54

Trethewey JA, Campbell LM, Harris PJ (2005) (1->3),(1->4)-beta-d-Glucans in the cell walls of the Poales (sensu lato): an immunogold labeling study using a monoclonal antibody. Am J Bot **92:** 1660–1674

Trethewey JAK, Harris PJ (2002) Location of (1→3)- and (1→3), (1→4)-beta-D-glucans in vegetative cell walls of barley (*Hordeum vulgare*) using immunogold labelling. New Phytol **154:** 347–358

Upadhyaya NM, Zhu QH, Zhou XR, Eamens AL, Hoque MS, Ramm K, Shivakkumar R, Smith KF, Pan ST, Li S, et al (2006) Dissociation (Ds) constructs, mapped Ds launch pads and a transiently-expressed transposase system suitable for localized insertional mutagenesis in rice. Theor Appl Genet **112:** 1326–1341

van Loon LC, Rep M, Pieterse CM (2006) Significance of inducible defense-related proteins in infected plants. Annu Rev Phytopathol **44:** 135–162

Verhertbruggen Y, Marcus SE, Haeger A, Verhoef R, Schols HA, McCleary BV, McKee L, Gilbert HJ, Knox JP (2009) Developmental complexity of arabinan polysaccharides and their processing in plant cell walls. Plant J **59:** 413–425

Vogel J (2008) Unique aspects of the grass cell wall. Curr Opin Plant Biol **11:** 301–307

Wang L, Guo K, Li Y, Tu Y, Hu H, Wang B, Cui X, Peng L (2010) Expression profiling and integrative analysis of the CESA/CSL superfamily in rice. BMC Plant Biol **10:** 282

Yin L, Verhertbruggen Y, Oikawa A, Manisseri C, Knierim B, Prak L, Jensen JK, Knox JP, Auer M, Willats WG, et al (2011) The cooperative activities of CSLD2, CSLD3, and CSLD5 are required for normal Arabidopsis development. Mol Plant **6:** 1024–1037